Copyright Warning & Restrictions

The copyright law of the United States (Title 17, United States Code) governs the making of photocopies or other reproductions of copyrighted material.

Under certain conditions specified in the law, libraries and archives are authorized to furnish a photocopy or other reproduction. One of these specified conditions is that the photocopy or reproduction is not to be "used for any purpose other than private study, scholarship, or research." If a, user makes a request for, or later uses, a photocopy or reproduction for purposes in excess of "fair use" that user may be liable for copyright infringement,

This institution reserves the right to refuse to accept a copying order if, in its judgment, fulfillment of the order would involve violation of copyright law.

Please Note: The author retains the copyright while the New Jersey Institute of Technology reserves the right to distribute this thesis or dissertation

Printing note: If you do not wish to print this page, then select "Pages from: first page # to: last page #" on the print dialog screen

ABSTRACT

INTENSE ULTRASONIC WAVES IN FLUIDS: NONLINEAR BEHAVIOUR

by
Jitendra Kewalramani

High-intensity ultrasonic wave has several engineering, biological, medical and chemical applications. High intensity acoustic waves can lead to a desired change in a medium by initiating one or more diverse mechanisms such as acoustic cavitation, heating, radiation pressure, or chemical reactions. Nonlinear nature of intense acoustic waves opens an entire new spectrum of applications. Hence there is need to understand and model the mechanism of nonlinear wave motion for practical applications of intense acoustic waves.

In this research, one-dimensional motion of shock waves in an ideal fluid is studied to include nonlinearity. In nonlinear acoustics, the propagation velocity of different sections of the waveform are different, which causes distortion in the waveform and results in formation of a shock (discontinuity). Intense acoustic pressure causes particles in fluid to move forward as if pushed by a piston to generate a shock. As the piston retracts, a rarefaction, a smooth fan zone of continuously changing pressure, density, and velocity, are generated. When the piston stops, another shock is sent into the medium. The wave speed can be calculated by solving a Riemann problem. This study examined the interaction of shocks with rarefactions. The flow field resulting from these interactions shows that the shock waves are attenuated to a Mach wave and the pressure distribution within the flow field shows the initial wave becoming severely distorted at a distance from the source. The developed theory was applied to waves generated by 20kHz, 500kHz and 2MHz transducer with 50W, 150W, 500W and 1500W power levels to examine the variation in flow fields.

INTENSE ULTRASONIC WAVES IN FLUIDS: NONLINEAR BEHAVIOUR

by
Jitendra Kewalramani

A Thesis
Submitted to the Faculty of
New Jersey Institute of Technology
in Partial Fulfillment of the Requirements for the Degree of
Master of Science in Civil Engineering

John A. Reif, Jr. Department of Civil and Environmental Engineering

May 2018

APPROVAL PAGE

INTENSE ULTRASONIC WAVES IN FLUIDS: NONLINEAR BEHAVIOUR

Jitendra Kewalramani

Dr. Jay N. Meegoda, Thesis Advisor — Date
Professor of Civil and Environmental Engineering, NJIT

Dr. Bruce Bukiet, Committee Member — Date
Associate Professor of Mathematical Sciences, NJIT

Dr. Lucia Rodriguez, Committee Member — Date
Assistant Professor of Civil and Environmental Engineering, NJIT

BIOGRAPHICAL SKETCH

Author: Jitendra Kewalramani

Degree: Master of Science

Date: May 2018

Undergraduate and Graduate Education:

- Master of Science in Civil Engineering,
  New Jersey Institute of Technology, Newark, NJ, 2018

- Bachelor of Engineering in Civil,
  The Maharaja Sayajirao University of Baroda, Gujarat, India 2016

Major: Civil Engineering

Publications:

Meegoda, J.N., Kewalramani, J.A., Saravanan, A., (2017). "Adapting 360-degree Cameras for Culvert Inspection" American Society of Civil Engineers (ASCE) Journal of Pipeline Systems- Engineering and Practice. Manuscript submitted for Publication.

To my parents

ACKNOWLEDGEMENT

This thesis would not have been possible without help and guidance of several people who have graciously contributed their time and expertise to not just competing this thesis but completing it well.

Firstly, and foremost, I would like to express my sincere gratitude to my advisor Professor Jay Meegoda for the continuous support of my thesis study and related research, for his patience, motivation, and immense knowledge. His guidance helped me in all the time of research and writing of this thesis. I could not have imagined having a better advisor and mentor for my thesis study.

I am grateful to Professor Bruce Bukiet for his interest in my work, for his fruitful ideas and discussions. He is my primary source of knowledge of nonlinear wave motion. I cordially thank, Professor Lucia Rodriguez for her participations, advice, encouragement and support. I also like to thank Dr. Zou Zhenting for his advice and guidance. I also like to thank Richard Marsh and Dana Channaoui for their help in mathematical calculation.

Last but not the least, I would like to thank my family: my parents and to my brother for supporting me spiritually throughout my studies and my life in general

TABLE OF CONTENTS

TABLE OF CONTENTS
(Continued)

LIST OF TABLES

LIST OF FIGURES

CHAPTER 1

INTRODUCTION

1.1 Objective

The appealing phenomena associated with intense, inaudible acoustic waves have the several scientific, engineering, industrial, chemical and medical applications and present a challenge in the fields of fundamental and applied mathematics (Gallego-Juárez & Graff, 2015). Ultrasonics is a branch of acoustics dealing with the generation and the applications of inaudible acoustic waves in various fields. In general, the field of ultrasonics can be divided into two broad areas: low-intensity applications and high-intensity applications. Ultrasonic non-destructive testing and the imaging used as means of exploration, detection, and information (e.g., the location of crack, material properties), are some of promising low-intensity applications. Generally low intensity applications are made at high frequencies, typically in megahertz range, and power level applied to transducer are typically low, often in the milliwatts ranges (Blitz, 1971).

High-intensity ultrasound is used to permanently change the physical, chemical, or biological properties or, if intense enough, even destroy the medium to which it is applied. The nonlinear phenomena associated with intense ultrasound wave opens an entire new spectrum of applications and can be broadly described as power ultrasonics (Gallego-Juárez & Graff, 2015). In the framework of nonlinear acoustics, familiar laws like the principle of superposition, reflection and rarefaction cease to be valid. One of the consequences of nonlinearity is the formation of shocks (discontinuities) in the waveform (Leighton, 2007). Applications of power ultrasonics is initiated by one or more diverse

mechanisms such as the wave distortion, radiation pressure, cavitation in liquids, heating, formation and motion of dislocations in solids etc. (Sapozhnikov, 2015). Intense ultrasonic waves can induce different processes in different media to an extent that they may be contradicting with each other (Gallego-Juárez & Graff, 2015). Known applications of this technology are the welding of metals and polymers, particle agglomerations, water and waste-water treatment, and the desorption of contaminates from soils and sediments (Gallego-Juárez & Graff, 2015; Meegoda, Batagoda, & Aluthgun-hewage, 2017). Understanding the basic mechanism of the nonlinear wave motion is essential for practical applications of intense acoustic waves and to develop new applications.

1.2 Sound Wave, Ultrasound Wave: A Review

A sound wave is the mechanical wave, which is a disturbance in a medium that transfers energy without requiring any net flow of mass. The speed of the wave is determined by the medium in which it is propagating, being directly related to stiffness and inversely related to density. The relationship between the speed of the wave and the wavelength can be expressed by the equation (1.1).

$$c = \lambda * f . \tag{1.1}$$

Ultrasound is a type of sound wave with frequencies ranging from 20kHz up to several gigahertz, higher than the upper limit of human hearing. Ultrasound is generated by the transducers which converts electrical energy into mechanical vibrations. Oscillations of the transducer causes particles in front of it to vibrate. Particles do not travel away from the transducer but are merely displaced locally. The oscillation of these particles creates acoustic waves, whose speed can be determined by the speed of the compressed region as it travels through the medium. In non-humid air at 20^0C, the speed of an acoustic

wave is 343m/s or 767mph. In the 1D model, the (maximum) speed of the oscillating particles in the acoustic field can be determined from displacement amplitude A and time period of wave T. The amplitude A can be defined as maximum displacement of particle from its equilibrium position in a medium and v is the maximum speed attained by particle can be calculated as follow: (Ghosh, 2013).

$$A = \sqrt{\frac{2I}{(\rho c)\omega^2}} \tag{1.2}$$

Where, $\omega = 2 * \pi * f$

$$v = A\omega = 2\pi f A \tag{1.3}$$

Where, I is the intensity of wave, f is the frequency, ρ is the density of medium and c is the sound speed in medium of propagation.

CHAPTER 2

ULTRASONIC APPLICATIONS

Ultrasonics is a branch of acoustics dealing with the generation and application of inaudible sound waves, corresponding to frequencies above 20kHz and ranges around 2MHz or higher, in various fields (Blitz, 1971). The first experimental studies of ultrasound go back to 1883, Mr. Galton found the upper limit of acoustic spectrum perceived by humans with help whistle, which can be regarded as one of the first man-made ultrasonic transducer (Blitz, 1971). Later in 1914-1918 during world war I, French scientist Langevin investigated use of quartz transducer for emitting and receiving ultrasonics waves, of relatively low frequencies in water, time delay between waves, provided means for detection of submarines (Hambling, 2017). The same technology give rise to ultrasonic nondestructive testing and imaging used as means for exploration, detection, and information. The key development to High-power ultrasonic came when Wood & Loomis, 1927, demonstrated the ranges of effect of intense ultrasonic waves such as induced drilling, atomization, levitation, heating of tissue, flocculation and crystallization (Gallego-Juárez & Graff, 2015). Ultrasound is used in preference to the audible sound in many applications for one or more of the following reasons: (Blitz, 1971)

- Directional Properties: Ultrasound wave travels in a straight line. This is main considerations in, for instance, crack detections and quality assurance of piles.
- Wavelength: As the frequency increases, wavelength correspondingly decreases and are comparable with, or even much less than, the dimensions of sample of material

through which it propagates. This is crucial for measurement of small thickness or for high-resolution flaw detections.

- Inaudible: This property advantageous for high-intensity applications. The applications such as water and waste-water treatment, and the desorption of contaminates from soil and sediments can be carried easily with audible frequencies but resulting noise may be intolerable and possibly injurious.

The Field of ultrasonics can be divided into two broad areas based on the power level of the transducers.

- Low-intensity applications
- High-intensity applications

It is difficult to establish limit between low and high intensity wave, but it can be approximated as 0.1 to 1 W/cm^2, depending upon medium propagation (Gallego-Juárez & Graff, 2015).

2.1 Low-Intensity Applications

Low intensity ultrasound is generally used for nondestructive testing and ultrasonic imaging as means of exploration, detection, and information. Most of low intensity applications are made at very high frequencies, typically in megahertz range, and power level applied to transducer are typically low, often in the milliwatt ranges (Blitz, 1971).

Ultrasound wave travels at a constant speed provided the disturbance caused by it in medium are purely elastic, i.e., acoustic intensity is low. Low intensity acoustic wave is useful for non-destructive defect analysis such as porosity, void, and delamination as well as analysis of material properties such as density, strength, and young's modulus. These

applications are based on techniques of measuring velocity and attenuation of the wave as it travels through the medium. In most of cases, a single instrument provides both these measurement, often simultaneously. The choice of frequency is based on various factors such as kind of information required from the measurement, size of sample, and by optimum sensitivity (Blitz, 1971).

2.1.1 Applications of Ultrasound to Structures

Nondestructive testing (NDT) methods are used to determine concrete properties and to evaluate concrete in deep foundations, bridges, buildings, pavements, dams, and other concrete construction. Ultrasonic Pulse Velocity (UPV) test can be effectively used for detecting the quality of concrete. The UPV test is easy to apply, it involves measurements of pulse velocity of wave (P-wave), a given path of pulse propagation over travel time (ACI 228.2R, 2013) . However, this method needs, access to both side of a structure. Moreover, wave transmission time is the only output of the UPV test and does not provide information on the depth of defects.

Ultrasound-echo method uses arrival time of stress wave (S-wave or transverse wave) reflected from a defect on one face of concrete structure to monitor concrete deterioration (ACI 228.2R, 2013). Recent advances have resulted in the improved transducer, array which can create a 3-D internal image of defects that are present in concrete (Bishko, Samokrutov, & Shevaldykin, 2008).

2.1.2 Applications of Ultrasound to Soil Properties

Handful studies were performed to demonstrate potential use of ultrasound to measure soil properties. Acoustic attenuation tends to increase in soil with increase in soil moisture, while speed is independent of soil moisture (Oelze, Darmody, & O'Brien, 2001). Collins,

Zhu, Mills, & Boxall, 2016, demonstrated an approach of using ultrasound reflection to study the soil water content beyond the pipe or culvert wall. Coe & Brandenberg, 2010, utilized ultrasonic p-wave reflection imagining system, to image the submerged soil model with embedded structural element. Evaluation of the acoustic propagation and scattering in soils to determine their index properties is being investigated.

2.2 High Intensity Applications

High intensity ultrasound or power ultrasonics is generally used to permanently alter the physical, chemical or biological properties of materials or systems. High-intensity applications are mostly made at low frequencies, usually in the ranges of 20kHz to 200kHz and acoustic power levels of 100W to 1000W. In some limiting applications, high-intensity method can be employed as non-destructive tests for example, submarine sonar, used to convey information. In general, ultrasound application can be defined as high intensity (or power ultrasonics), when the acoustic stresses developed are sufficiently great to result in a nonlinear strain, ceasing to obey the Hooke's law. Applications of power ultrasonics are initiated by one or more diverse mechanism such as wave distortion, radiation pressure, cavitation in liquids, formation and motion of dislocations in solids etc.

Intense ultrasonic waves can induce different phenomena in different media, depending on type of medium, to an extend that may be contradict to each other. For instance, intense ultrasound can create particle dispersion to liquid suspension, whereas, its application to gas suspension leads to particle agglomeration (Gallego-Juárez & Graff, 2015). Known applications of this technology are the welding of metals and polymers, particle agglomerations, water and waste-water treatment, and the desorption of contaminates from soil and sediment(Gallego-Juárez & Graff, 2015; Meegoda et al., 2017).

In the following section application involving the propagation of ultrasound in liquid medium are described.

2.2.1 Water Treatment

The propagation of intense ultrasonic wave can be used to eliminate pollutants from water. The classical treatment methods used for drinking water treatment do not always result in water that meet the current regulatory requirements. Advanced Oxidation Processes (AOPs) have been developed to improve efficiency of water treatment (Glaze, Kang, & Chapin, 1987). AOPs involves the production and use of the hydroxyl radical ·OH, which eliminate the organic and mineral pollutants by oxidizing them. The radical can be produced by various ways such as (1) The propagation of ultrasound, (2) electrochemistry, (3) Ozone and hydrogen peroxide, (4) UV irradiations, (5) ozone photodecomposition etc., (Parson & Williams, 2004).

In the ultrasonic process, the generation of hydroxyl radicals ·OH are not due to interaction between the acoustic waves and aqueous liquid, but are formed from the pulsation and collapse of cavitation bubbles, created from the pressure change resulting from propagation of wave in the liquid (Petrier, 2015). Cavitation bubbles grow from the smaller bubbles containing dissolved gases and water vapor that are expelled from crevices on the surface of suspended solid particles. Following a periodical change in the pressure, the tiny bubbles pulsate, with their diameter increases during expansions and decreases as the pressure is increased.

Acoustic waves are the longitudinal waves, generated by the vibration of transducers. As the transducer is moving back and forth, it pushes the neighboring fluid

particles. The forward motion of transducer pushes fluid particle to the right (propagation direction of wave) and the backward retraction of the transducer creates a low-pressure area allowing the fluid particle to move back to left. Due to longitudinal motion of fluid particles, there will be regions in the fluid where fluid particles are compressed together and other regions where fluid particle are spread apart. These regions are known as compression and rarefactions respectively. The compression are the regions of high pressure while the rarefaction are regions of low pressure.

During the low-pressure (rarefaction) of the pulse, there is entry of dissolved gases and water vapors to maintain the equilibrium of vapor pressure inside the bubble. Conversely, during the high-pressure (compression) of the pulse there is dissolution of gases from bubbles to the medium and liquification vapor pressure. The rate of this process is related to surface area of the bubble as it is the transfer surface of gases from and to the bubble. The bubble expansion associated with low pressure cycle of pulse is the dominant process, as surface area of bubble is higher. As a result, bubble size increases. This growth is not limitless, as bubble can collide with other, or the bubbles can reach a critical size and collapse at the beginning of compression side of pulse. Under such conditions, there is adiabatic compression of gases and vapors to a very high temperature (Petrier, 2015). The energy of collapse drives the inside material in the bubble to a plasma state, instantaneously achieving very high temperatures and pressures.

It is postulated, in extreme temperature and pressures, water and oxygen molecules can be driven into the exited state of atoms and molecules and dissociate into hydroxyl, hydrogen and oxygen radicals, according with following equation (Henglein, 1987).

$$H_2O \longrightarrow {}^{\cdot}OH + H^+ \quad (2.1)$$

$$O_2 \longrightarrow 2O^- \quad (2.2)$$

Hydroxyl radical's formation react and combine in different ways in the final condensed phase of the collapse. Involvement of the ·OH radical in oxidative chemical reaction by ultrasonic waves have received considerable attention and is well established (Henglein, 1987). These phenomena of ultrasonic cavitation lead to the destruction of organic pollutant through thermal oxidation.

The scheme published by Segal and Wang (1981), as shown in figure 2.1 can be used to approximate the location of reaction. Radicals generated in the gaseous phase in the bubble react in the condensed layer at the liquid interface. This interface accumulates organic molecules depending on their hydrophobic characteristics. The more hydrophobic the structure (of organic pollutant) the greater the accumulation of those at the interface, the more it reacts with the hydroxyl radicals coming from the inside, and the more rapid degradation (Sivasankar & Moholkar, 2009).

Another mechanism for pollutant degradation is the pyrolysis due to the high temperatures the cavitation during ultrasound application can be considered as a microreactor that incinerates volatile molecules at high temperatures when the bubble collapse (Petrier, 2015). When two kinds of molecules are present (volatile and nonvolatile molecules) together in aerated water, first volatile molecules are oxidized eliminated and then nonvolatile are oxidized.

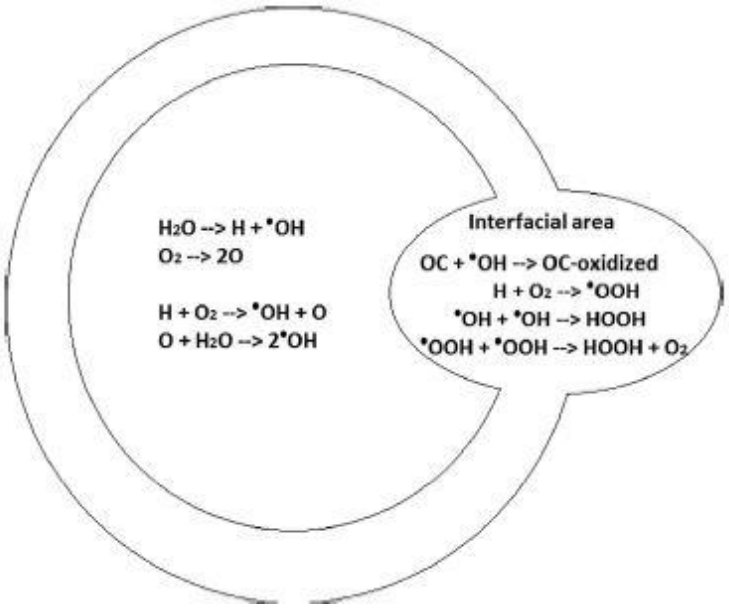

FIGURE 2.1 Scheme of Reaction Occurring in and at the Interface of Bubble. Accounting for the hydrophobic organic compound (OC) oxidation.

Source:(Sehgal & Wang, 1981)

Although sonochemical treatment can eliminate most organic water pollutants, the efficiency depends on various factors. Key factor is the frequency of source. The diffusion of ultrasonic wave depends upon the ratio of λ/D, where λ is the wavelength and D is the diameter of probe. For low frequency probe, most of energy, and the subsequent cavitation, occurs in the small volume close to the surface of probe (20kHz -40kHz) (Petrier, 2015). Ultrasound energy is more dispersed in volume of reactor with a high frequency transducer. The high frequency system works as well-stirred reactors. The use of ultrasonic waves of frequency range above 200kHz leads to an increased degradation of organic pollutants than can be achieved with a low frequency range. As the size of the collapsing bubbles and the duration of the collapse decrease with frequency, these improves the availability of hydroxyl radicals (˙OH) at the interface of bubbles improving the degradation of organic pollutants (Christian Petrier et al., 1994).

2.2.2 Wastewater Treatment

It was recognized in early 1990, that the innovative technology of high intensity ultrasound can improve the traditional anaerobic reaction of organic sludge produced during waste-water treatment (Neis, 2015). Wastewater activated sludge consist of highly concentrated bacterial cells held together by extracellular substances in a floc structure. The idea behind using the intense ultrasound is to disintegrate sludge cells (de-agglomerate) and subsequently intensify the anaerobic degradation, eventually resulting in more biogas and less residual sludge. The following effects of propagating intense ultrasound in waste water sludge can improve the anaerobic degradation.

- Alternating zone of compression and rarefaction
- Acoustically induced cavitation causing high mechanical stresses and radical reactions (such as sonochemical reactions).

In such a process, usually low frequency ultrasound, sufficient for de-agglomeration is generally applied. At high intensities, microorganism cell walls are broken or perforated, and intracellular material is released, resulting in increase in the amount of organic material (Tiehm, Nickel, & Neis, 2001). The applications of power ultrasound for the disintegrations and intensification of anaerobic digestion is well established, however a rational design procedure for reactors is still lacking, and today's reactors are designed empirically.

CHAPTER 3

NONLINEAR ACOUSTICS

In the linear wave motion, sound wave propagate at a constant speed (relative to the medium), and do not influence the fluid. If wave intensity is increased, this situation dramatically changes, wave starts experiencing nonlinearity (Sapozhnikov, 2015). In nonlinear acoustics, propagation speed of different regions of waveform are different, which causes distortion in waveform and results in formation of shock (discontinuities) in the waveform (Blackstock, et al., 1998). As Shown in figure 3.1 Shock formation corresponds to the transformation of waveform from sinusoidal to a sawtooth shape (called as N-wave). With the shocks, a jump condition is formed between the fluid in front and the volume behind the shock (Courant & Friedrichs, 1948).

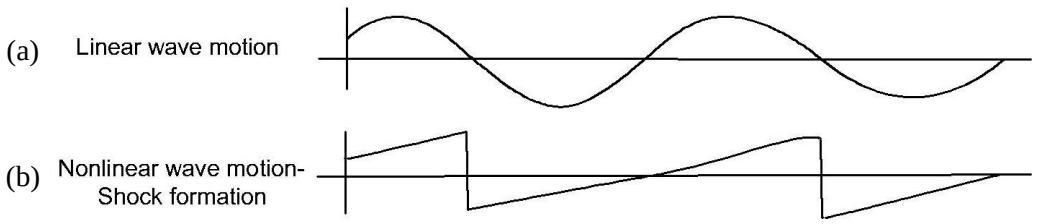

FIGURE 3.1: Schematic of Linear and Nonlinear Wave Motion. (a) Unlike the low-intensity ultrasonic wave propagating linearly (b) high-intensity ultrasonic wave propagate nonlinearly, such that as it propagates away from source, the waveform gets distorted and results in formation of shock in the waveform.

Source:(Leighton, 2007).

3.1 Linear & Nonlinear Wave Motion

The nonlinear wave motion can be described using the principle of the linear theory of acoustics (Sapozhnikov, 2015). In linear wave motion, consider an undisturbed medium ($u = 0$) characterized by the thermodynamic variables density ρ_0, pressure P_0, entropy S_0, and temperature T_0,. A disturbance u in the medium is characterized by the perturbations

$$\rho' = \rho - \rho_0 \tag{3.1}$$

$$P' = P - P_0 \tag{3.2}$$

$$S' = S - S_0 \tag{3.3}$$

$$T' = T - T_0 \tag{3.4}$$

Perturbations of density (ρ') and temperature (T') can be expressed through the perturbations of pressure (P') and entropy (S') using the thermodynamic relations (Sapozhnikov, 2015). Therefore, only three variables, $u, P', and\ S'$, are needed to determine the linear wave motion.

The perturbations can be defined as a result of three independent modes: acoustic, entropy, and vorticity modes, where $u = u_{vor} + u_{ac} + u_{ent},\ P' = P_{vor} + P_{ac} + P_{ent}$ and so on respectively (Pierce, 1994). In the vorticity mode, only the velocity (u_{vor}) is disturbed, whereas the other thermodynamic variables ($e.g.,\ P_{vor},\ S_{vor}$) remain in their equilibrium state (Pierce, 2002; Sapozhnikov, 2015). In the Acoustic mode associated with the sound wave, the viscosity, thermal conductivity, and entropy perturbations (S_{ac}) are zero, and the perturbations of density (ρ_{ac}) and temperature (T_{ac}) can be expressed through the pressure perturbations (P_{ac}) (Pierce, 2002; Sapozhnikov, 2015). The entropy mode describes the heat transfer, where entropy fluctuations (S_{ent}) are significant in this

mode, whereas the pressure perturbation (P_{ent}) is nearly zero, the perturbations of density (ρ_{ent}) and temperature (T_{ent}) can be expressed in terms of entropy perturbations (Sapozhnikov, 2015).

As the speed of the disturbance increases, linear wave motion cease, therefore superposition principle is no longer valid, thus disturbance cannot be described in form of three independent modes (Pierce, 2002). These modes start interacting with one another. Three interactions between these modes are activated in the nonlinear propagation of the acoustic wave: the sound-sound, sound-vorticity and sound-entropy interactions (see Figure 3.2) (Pierce, 2002).

During propagation of the intense acoustic waves, first due to the sound-sound interactions, harmonic generations and self-demodulations occur within acoustic mode (Pierce, 2002). Then, acoustic mode starts to interact with other two modes, this interaction includes acoustically induced heating and generation of hydrodynamic flow (Pierce, 2002).

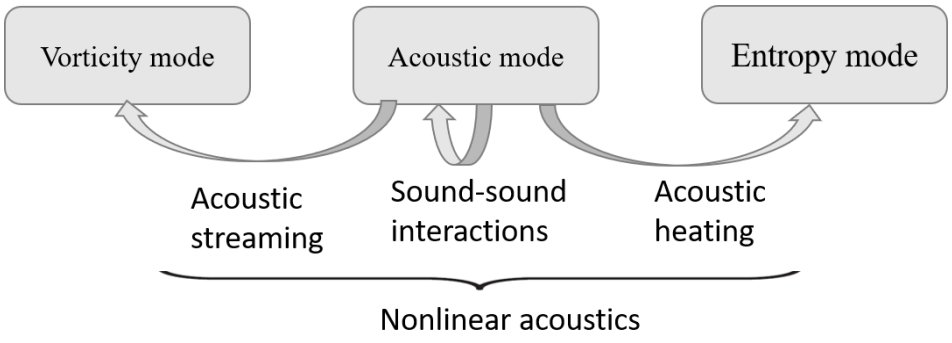

FIGURE 3.2 Study of Nonlinear Acoustics. For power ultrasonics, flow fields can be describe using the three basic modes of fluctuations with those modes interacting with each other and with themselves.

Source:(Sapozhnikov, 2015).

3.2 Nonlinear Propagation & Shock Formation

In the framework of the linear wave motion, acoustic waves are presumed to propagate in a thermoviscous fluid at constant speed. However, at the higher ultrasonic intensities, and frequencies, the disturbance u in medium can be sufficiently high that nonlinear propagation occur (Leighton, 2007). A Consequence of this result is the fact that local sound speed c depends on the disturbance speed u (c as function of u), c_u, so does the local wave propagation velocity gets modified to $c_u + u$ (Sapozhnikov, 2015). There are two independent sources of the acoustic nonlinearity.

- Change of the wave propagation speed due to drift with velocity u.
- Change in local sound speed from c_0 to c_u.

Thus, transition from linear regime to a nonlinear one corresponds to the change $c_0 \longrightarrow c_u + u$. Wave propagation speed varies throughout the waveform, and so the greater the local acoustic pressure, greater the local wave speed. As shown in figure 3.3, during nonlinear propagation, region of the compression (where u and c_u are in same direction), would tends to travel at speed faster than the region of the expansion (where u is opposite to c_u). Thus, a continuous waveform that is initially sinusoidal will therefore gets distorted as it progresses from the source. As a consequence of nonlinear distortion, there is formation of the shock (discontinuity) in the waveform (Blackstock & Hamilton, 1998; Courant & Friedrichs, 1948). At the shock, the jump condition is form and the medium undergoes abrupt, and nearly discontinuous change in the pressure, density and temperature. Nonlinear distortion accumulates gradually during wave propagation. Therefore, shock appear at some distance from source.

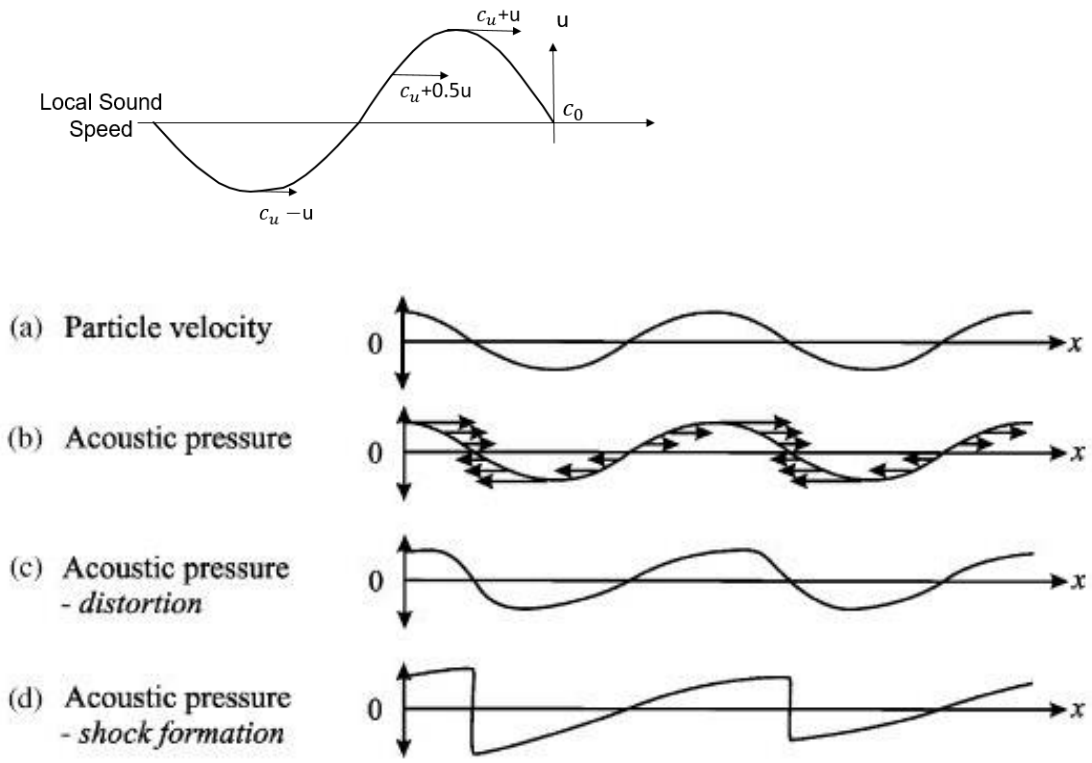

Figure 3.3 Schematic Representation of Acoustic Distortion and Shock Formation during Nonlinear Propagation. The upper sketch is a spatial plot of the initial waveform (t=0). The first two graph shows the initial sinusoidal waveform in terms of (a) particle velocity and (b) pressure at various distances x. Unlike linear propagation of the wave, these waveforms propagate nonlinearly, such that as it propagates from the source, the pressure waveform distorts (c), and if dissipation is not too great, can eventually form a shock.

Source (Blackstock & Hamilton, 1998; Leighton, 2007)

3.3 Nonlinear Interactions within Acoustic Mode

The simplest way to describe the nonlinear behavior of intense ultrasound waves is to consider the one-dimensional motion of an ideal fluid, where it has no viscosity or thermal conductivity. In this case, $v = (u, 0,0)$ and all variables depend only on *x* and *t*. The motion of the wave can be modeled as the flow of an ideal fluid in an infinitely long tube extending along the x-axis, with one end having a moving piston and the other end as fixed wall. In one-dimensional model, nonlinear waves are propagating only in one direction.

In a gas-filled tube, if a piston is moved into or if a receding piston is stopped a shock (discontinuities) is generated, that moves away from the piston. Similarly, a rarefaction wave is sent into medium when the piston recedes away from the fluid (Courant & Friedrichs, 1948). In this case of rarefaction wave, not all the regions of the wave are affected simultaneously, only the particles impacted by wave are disturbed from their initial state. A pulse ultrasonic wave can be conceived as one complete cycle of piston in tube. That is, piston moves from a stationary, or at rest position at a constant speed until it reaches the maximum point of displacement, stops instantaneously and reverse the direction, moves in the opposite direction at the same speed as the propagation velocity and stops at the rest location. As shown in figure 3.4, there will be a shock originated as the piston moves forward, a rarefaction wave sent as advancing piston stops and starts receding and another discontinuity originate at tail of the cycle.

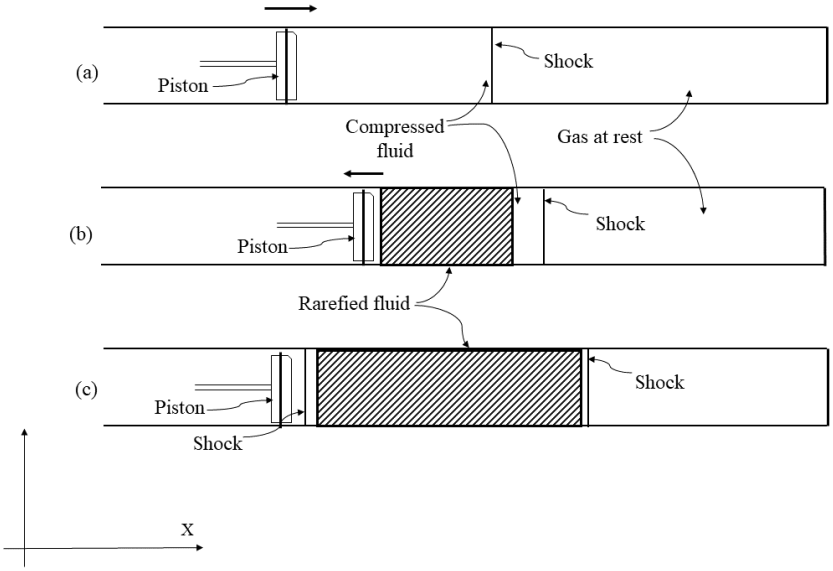

FIGURE 3.4 Generation of Shock and Rarefaction Wave. (a) Shock produced by a piston moving with constant velocity into the fluid at rest. (b) As the piston reaches its maximum displacement and changes the direction of propagation a rarefaction wave is sent into the compressed fluid behind the shock. (c) When piston comes to rest, another shock is produced.
Source (Courant & Friedrichs, 1948).

The one-dimensional flow eliminates the vorticity mode, and absence of dissipations makes the process adiabatic, that is, it excludes the entropy modes as well. Therefore, above equations only describe nonlinear behavior of the acoustic mode (Sapozhnikov, 2015).

The propagation of intense acoustic wave in one-dimensional motion can be mathematically described by using the conservation equation of mass, momentum and energy:

$$\begin{pmatrix} \rho \\ m \\ e \end{pmatrix}_t + \nabla * \begin{pmatrix} m \\ \frac{m^2}{\rho} + P \\ \left(\frac{m}{\rho}\right)(e + P) \end{pmatrix} = 0 \tag{3.5}$$

Here ρ is the density of gas, m is the momentum, P is the pressure and e is the energy per unit volume which is expressed as:

$$e = \rho\varepsilon + \frac{\rho u^2}{2} \tag{3.6}$$

Here u is the particle velocity and specific internal energy ε is:

$$\varepsilon = \frac{P}{\rho(\gamma - 1)} \tag{3.7}$$

With shock speed U, the conservation of mass can be written as:

$$\rho_1(u_1 - U) = \rho_0(u_0 - U) \tag{3.8}$$

The subscripts 0 and 1 represent the states ahead of and behind the shock. The conservation of momentum for the shock can be expressed as:

$$\rho_1(u_1 - U)^2 + P_1 = \rho_0(u_0 - U)^2 + P_0 \tag{3.9}$$

The conservation of energy for the shock can be written as:

$$(u_1 - U)(e_1 + P_1) = (u_0 - U)(e_0 + P_0) \tag{3.10}$$

By using the specific volume, $\tau = 1/\rho$, equations $(3.8), (3.9) and\ (3.10)$ can be reduced to the Hugoniot relation (Bukiet, 1988):

$$\frac{\gamma_0 \tau_0 P_0}{\gamma_0 - 1} - \frac{\gamma_1 \tau_1 P_1}{\gamma_1 - 1} = \frac{(P_0 - P_1)(\tau_0 + \tau_1)}{2} \tag{3.11}$$

3.4 Riemann Problem

Equations (3.8) – (3.10) describe nonlinear behavior of the acoustic mode alone. Riemann showed a long time ago these equations can have an exact general solution in the form of the waves. To solve the Riemann problem, initial data can be described as follow:

$$S_L = (\rho_L, u_L, P_L) for\ Left\ wave\ (x < 0) \tag{3.12}$$

$$S_R = (\rho_R, u_R, P_R) for\ Right\ wave\ (x > 0) \tag{3.13}$$

By using this initial data, the solution would consist of a right wave, a left wave and a contact. Right (or left) wave can be a shock or a rarefaction as shown in figure 3.5.

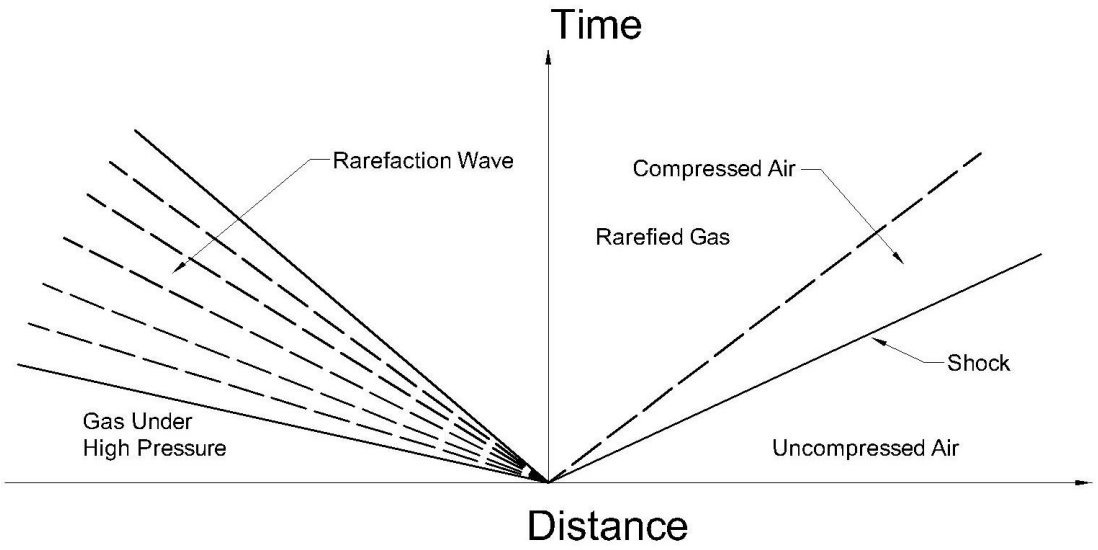

FIGURE 3.5 Riemann Solution for Wave Motion. Resulting flow field generally consist of a left-facing wave and a right-facing wave that can be a shock or rarefaction, separated by a contact discontinuity.

Source (Courant & Friedrichs, 1948)

Intermediate region can be connected to left or right regions by following Riemann invariants (Bukiet, 1988):

$$\frac{u_L}{2} + \frac{c_L}{\gamma_L - 1} = \frac{u_*}{2} + \frac{c_*}{\gamma_* - 1} \tag{3.14}$$

$$\frac{u_R}{2} + \frac{c_R}{\gamma_R - 1} = \frac{u_*}{2} + \frac{c_*}{\gamma_* - 1} \tag{3.15}$$

Using the isentropic law, the following is obtained:

$$P_L {\rho_L}^{-\gamma_L} = P_* {\rho_*}^{-\gamma_*} \tag{3.16}$$

$$P_R {\rho_R}^{-\gamma_R} = P_* {\rho_*}^{-\gamma_*} \tag{3.17}$$

Here * denotes the region inside the wave, or mid-region. Equations for shock or rarefaction wave can be found by eliminating U and ρ_1 from equations (3.8) – (3.10). Since left and right regions connect to regions with same velocity and pressure, equations can be expressed in terms of velocity as a function of pressure (Bukiet, 1988). Newton's iteration scheme is used to solve the equation for the velocity and pressure of the mid-region. Bukit, 1988, presented the following equations, relating the intermediate state of wave to side state:

Right shock:

$$u = u_R + \frac{A_R(\alpha_R - 1)}{(D_R\alpha_R + E_R)^{1/2}}, \frac{du}{dP} = \frac{\alpha_R D_R + 3\gamma_R - 1}{\sqrt{2\rho_R P_R}(D_R\alpha_R + E_R)^{3/2}} \tag{3.18}$$

Right rarefaction:

$$u = u_R + \frac{2C_R({\alpha_R}^{B_R} - 1)}{E_R}, \frac{du}{dP} = \frac{1}{H_R {\alpha_R}^{J_R}} \tag{3.19}$$

With:

$\alpha_S = \frac{P}{P_S}$; $A_S = \sqrt{\frac{2P_S}{\rho_S}}$; $B_S = \frac{\gamma_S - 1}{2\gamma_S}$; $C_S = \sqrt{\frac{\gamma_S P_S}{\rho_S}}$; $D_S = \gamma_S + 1$; $E_S = \gamma_S - 1$;

Here S is the side, R and L denote the region of fluid to the right or left side of mid-region. Equations (3.8) and (3.11) can be used to compute mid-region density and wave speed for shock, while equations (3.14) - (3.17) can be used for rarefactions.

3.4.1 Head Shock

With the one-dimensional model, as high intense ultrasound wave is sent into medium, it will push fluid in front (like a piston) and a shock is generated. As mentioned before, a nonlinear wave is propagating in one direction only, assuming the direction of propagation as right, so the right shock equation can be used. To demonstrate the calculations, following parameters for ultrasound transducer were assumed:

Transducer of $1500W$, 80% efficiency, source diameter of 12.7mm, frequency of 2MHz and, ideal fluid, $\rho = 1.225\, kg/m^3$, $c_0 = 343m/s$.

Using equation (1.2) and (1.3).

$$A = \sqrt{\frac{2I}{(\rho c)\omega^2}}$$

$$= \sqrt{\frac{2 * (.8 * 1500)/(3.14 * .25 * (12.7 * 10^{-3})^2}{(1.225 * 343) * 12560000^2}}$$

$$= 1.691 * 10^{-5}m$$

$$\omega = 2 * \pi * f = 2 * 3.14 * 2 * 10^6 = 12560000Hz$$

$$u = 2 * A * f * \pi = 1.691 * 10^{-5} * 12560000 \approx 212.4m/s$$

In the front of the head shock fluid is in undisturbed state, particle speed is 0m/s and behind the shock particle speed is 212.4m/s. Using equation (3.18), to calculate the pressure behind the shock, in the expression subscript “1” and “r1” represent fluid, ahead and behind of shock respectively. Thereby, u_1 is equal 0m/s, as the fluid in front of the

head shock is undisturbed. The P_1, normal fluid pressure is equal to the 101,325Pa, ρ_1 is equal to the 1.225kg/m^3 and specific heat ratio γ for normal fluid equals is 1.4, unknown P_{r1} can be calculated as:

$$u_{r1} = \mathrm{u}_1 + \frac{\sqrt{\frac{2\mathrm{P}_1}{\rho_1}}\left(\frac{P_{r1}}{\mathrm{P}_1} - 1\right)}{\left[\left\{(\gamma+1)\frac{P_{r1}}{\mathrm{P}_1}\right\} + (\gamma-1)\right]^{1/2}}$$

$$212.4 = 0 + \frac{\sqrt{\frac{2 * 101325}{1.225}}\left(\frac{P_{r1}}{101325} - 1\right)}{\left[(1.4+1)\frac{P_{r1}}{101325} + (1.4-1)\right]^{1/2}}$$

$$P_{r1} = 229{,}029Pa \; or \; 40{,}530Pa$$

For the propagation direction, particle speed u_{r1} and sound speed c_{r1} are in same direction, thus, $P_{r1} > P_1$, thus, P_{r1} value of 229,029Pa is selected. Equation (3.8) and (3.11) can be used to calculate shock speed and density behind the shock

Using Hugoniot equations (3.11):

$$\frac{1.4 * \left({}^{1}/_{1.225}\right) * 101325}{1.4-1} - \frac{1.4 * \left({}^{1}/_{\rho_{r1}}\right) * 229029}{1.4-1}$$

$$= \frac{(101325 - 229029)\left(\left({}^{1}/_{1.225}\right) + \left({}^{1}/_{\rho_{r1}}\right)\right)}{2}$$

$$\rho_{r1} = 2.16kg/m^3$$

With the conservation of mass, equation (3.8):

$$2.16(212.4 - U_1) = 1.225(0 - U_1)$$

$$U_1 = 490.8m/s$$

By applying the Hugoniot relationship density behind the head shock is equals to 2.16kg/m^3. The speed of shock generated by the vibration speed of particle as 212.4m/s is

490.8m/s. Shocks always moves at a supersonic speed as observed on front side, and subsonic speed as observed from back side.

3.4.2 Rarefaction

During the wave propagation, fluid particles are vibrating back and forth in direction of the propagation around its original position (like an oscillating piston). Once the direction of motion of fluid particles changes, a rarefaction is generated. Rarefaction is a smooth fan zone with continuously changing pressure, density and velocity. Subscript $r1$ and $r2$ represent face and tail of rarefaction. The particle velocity of the face rarefaction is $u_{r1} = 212.4m/s$. As fluid particles recede, piston velocity become negative, $u_{r2} = -212.4m/s$ and a rarefaction wave is sent to the system. Using equation (3.19) for right rarefaction, where, $\mathrm{u_{r1}} = 212.4\mathrm{m/s}$, speed attained by particle at edge of piston with $P_{r1} = 229029\mathrm{Pa}$ and $\rho_{r1} = 2.16kg/m^3$, P_{r2} pressure at tail of rarefaction can be calculated:

$$u_{r2} = u_{r1} + \frac{2\sqrt{\frac{\gamma * P_{r1}}{\rho_{r1}}}\left(\left(\frac{P_{r2}}{P_{r1}}\right)^{\frac{\gamma-1}{2\gamma}} - 1\right)}{\gamma - 1}$$

$$-212.4 = 212.4 + \frac{2\sqrt{\frac{1.4 * 229029}{2.16}}\left(\left(\frac{\mathrm{P_{r2}}}{229029}\right)^{\frac{1.4-1}{2*1.4}} - 1\right)}{1.4 - 1}$$

$$\mathrm{P_{r2}} = 40{,}055Pa$$

For the rarefaction wave, as particle speed u_{r2} and sound speed c_{r2} are in opposite direction, and acoustic pressure, $\mathrm{P_{r2}} < P_1$.

Equation (3.15) and (3.16) is used to determine density at tail of rarefaction wave,

$$P_{r2}\rho_{r2}{}^{-\gamma_R} = P_{r1}\rho_{r1}{}^{-\gamma_*}$$

$$40055 * \rho_{r2}{}^{-1.4} = 229029 * 2.16^{-1.4}$$

$$\rho_{r2} = 0.62\text{kg/m}^3$$

As mentioned, transition from linear to nonlinear regime corresponds to change in propagation velocity from $c_0\ to\ u + c$. Using this and data from the shock speed calculations, the wave velocity at face of rarefaction is equal to $u_{r1} + c_{r1} = 212.4 + \sqrt{\frac{1.4*229029}{2.16}} = 212.4 + 385.69 = 597.68 \approx 597.7\text{m/s}$, which is faster than the head shock speed, also the propagation speed at tail of rarefaction wave would be $-u_{r2} + c_{r2} = -212.4 + \sqrt{\frac{1.4*40055}{0.62}} = -212.4 + 300.74 = 88.34 \approx 88.3\text{m/s}$. With front and tail of the rarefaction known, and it can help to compute the intermediate point in the rarefaction (Zhenting , 2017).

To compute the intermediate regions in rarefaction, assume constant $k1$, $k2$, and $k3$:

$$k1 = \frac{dx}{dt} = u_* + c_* \tag{3.20}$$

$$k2 = \frac{u_{r1}}{2} - \frac{c_{r1}}{\gamma - 1} = \frac{u_*}{2} - \frac{c_*}{\gamma - 1} \tag{3.21}$$

$$k3 = P_{r1}\rho_{r1}{}^{-\gamma} = P_*\rho_*{}^{-\gamma} \tag{3.22}$$

k1, k2 and k3 can be related as follow, let k1 minus two k2 to get:

$$k1 - 2 * k2 = 6\sqrt{1.4 * \frac{P_*}{\rho_*}} \tag{3.23}$$

From Equation (3.22),

$$P_* = k3 * \rho_*^{1.4} \tag{3.24}$$

Substitute P_* in (3.23) by using (3.24) to obtain:

$$\rho_* = \left[\frac{\left(\frac{k1 - 2k2}{6}\right)^2}{1.4k3}\right]^{2.5} \tag{3.25}$$

Here k2 and k3 are constant, there by knowing the state at the of front rarefaction and by using different values of k1, the density of each point in the rarefaction can be found. Then, using (3.25) and (3.17), the pressure for point in the rarefaction can be calculated as shown below:

$$P_* = \frac{P_{r1} * {\rho_*}^{1.4}}{\rho_{r1}^{1.4}} \tag{3.26}$$

Finally, the particle velocity of the rarefaction can be determined by using (3.15).

$$u_* = 2 * \left[\left(\frac{u_{r1}}{2} - \frac{C_{r1}}{\gamma - 1}\right) + \frac{c_*}{\gamma - 1}\right] \tag{3.27}$$

Due to the smooth change in velocity in the rarefaction, the k1 has its own velocity range between the tail rarefaction velocity of 88.3m/s and the face rarefaction velocity 597.7m/s. Consequently, k2 and k3 can be calculated as

$$k2 = \frac{u_{r1}}{2} - \frac{C_{r1}}{\gamma - 1} = -857m/s$$

$$k3 = P_{r1}{\rho_{r1}}^{-\gamma} = 77944m/s$$

Rarefaction wave can be divided into two parts separated by sound wave, where $u_* + c_* = c_0$ (Courant & Friedrichs, 1948). Let ρ_r, P_r represent the density and pressure at separation boundary respectively, using $K_1 = u_r + c_r = 343m/s$, and equations (3.25) and (3.26) to find separation boundary.

$$\rho_r = \left[\frac{\left(\frac{343 + 2 * 857}{6}\right)^2}{1.4 * 77944}\right]^{2.5} = 1.2kg/m^3$$

$$P_r = \frac{229029 * 1.2^{1.4}}{2.16^{1.4}} = 101{,}161.4Pa$$

Thus, rarefaction can be divided into two zones at boundary, $P_r = 101{,}161.4Pa, and\ \rho_r = 1.2kg/m^3$.

3.4.3 Tail Shock

At the end of pulse wave, as fluid particle will come to rest, particle speed will change from -212.4m/s to 0m/s, and another shock will be generated. Using equation (3.18), to calculate the pressure behind the tail shock, in the expression subscript "r2" and "2" represent fluid, ahead and behind of shock, respectively. u_2 is the particle velocity behind the tail shock which equals to $0\ m/s$, u_{r2} is equal $-212.4\ m/s$, P_{r1} is $40{,}055Pa$, ρ_{r2} is 0.62 kg/m^3, and γ for normal air equals to 1.4. Substituting these values into equation (3.18), unknown P_2 can be calculated:

$$u_2 = \mathrm{u}_{r2} + \frac{\sqrt{\frac{2\mathrm{P}_{r2}}{\rho_{r2}}}\left(\frac{P_2}{\mathrm{P}_{r2}} - 1\right)}{\left[\left\{(\gamma_r + 1)\frac{P_2}{\mathrm{P}_{r2}}\right\} + (\gamma - 1)\right]^{1/2}}$$

$$0 = -212.4 + \frac{\sqrt{\frac{2 * 40055}{0.62}}\left(\frac{P_2}{40055} - 1\right)}{\left[(1.4 + 1)\frac{P_2}{40055} + (1.4 - 1)\right]^{1/2}}$$

$$P_2 = 99{,}954Pa$$

Using Hugoniot expression (3.11) to calculate density at shock.

$$\frac{1.4 * \left({}^{1}/_{0.62}\right) * 40055}{1.4 - 1} - \frac{1.4 * \left({}^{1}/_{\rho_2}\right) * 99954}{1.4 - 1}$$

$$= \frac{(40055 - 99954)\left(\left({}^{1}/_{0.62}\right) + \left({}^{1}/_{\rho_2}\right)\right)}{2}$$

$$\rho_2 = 1.38 kg/m^3$$

With the conservation of mass, equation (3.8):

$$1.38(0 - U_1) = 0.62(-212.4 - U_2)$$

$$U_2 = 172.4 m/s$$

By applying the Hugoniot relation, the density behind the tail shock equals to 1.38kg/m^3 and the tail shock speed is 172.4m/s.

3.5 Decaying of N-Wave

In a pulse of ultrasonic wave, there will be two shocks and a rarefaction in between. The velocity of head shock is subsonic relative to local sound speed behind. Thus, a rarefaction wave eventually overtakes the head shock causing shock to weaken. Similarly, as shock velocity is supersonic relative to local sound speed ahead of it, tail shock will eventually overtake the rarefaction wave. The rarefaction can be divided into two parts, separated by wave speed of sound, where $u_* + c_* = c_0$. The head shock traverses the forward part of the rarefaction and the tail shock crosses the backward part (Courant & Friedrichs, 1948).

Speed of waveform at face of rarefaction is $u_{r1} + c_{r1} = 597.7 m/s$,whereas speed of head shock is $U_1 = 490.8 m/s$, thus after some time rarefaction will overtake the head shock. Similarly, the speed of waveform at tail of rarefaction is $u_{r2} + c_{r2} = 88.3 m/s$, for tail shock is $U_2 = 172.4 m/s$, so tail shock will be overtaken from backward rarefaction waveform, as shown in figure 3.6.

Back in 1950s, extensive experimental investigations were performed at Institute of Aerophysics, University of Toronto (which was earlier known as Institute of Aerospace Studies) on flow field resulting from one-dimensional wave interactions, two studies namely overtaking of shock by a rarefaction wave by Glass, et.al., 1959 and another study on one-dimensional shock overtaking rarefaction wave by Bermner, et.al., 1960 can be used to study the interaction between head shock and forward part of refraction wave and tail shock and backward part of rarefaction respectively.

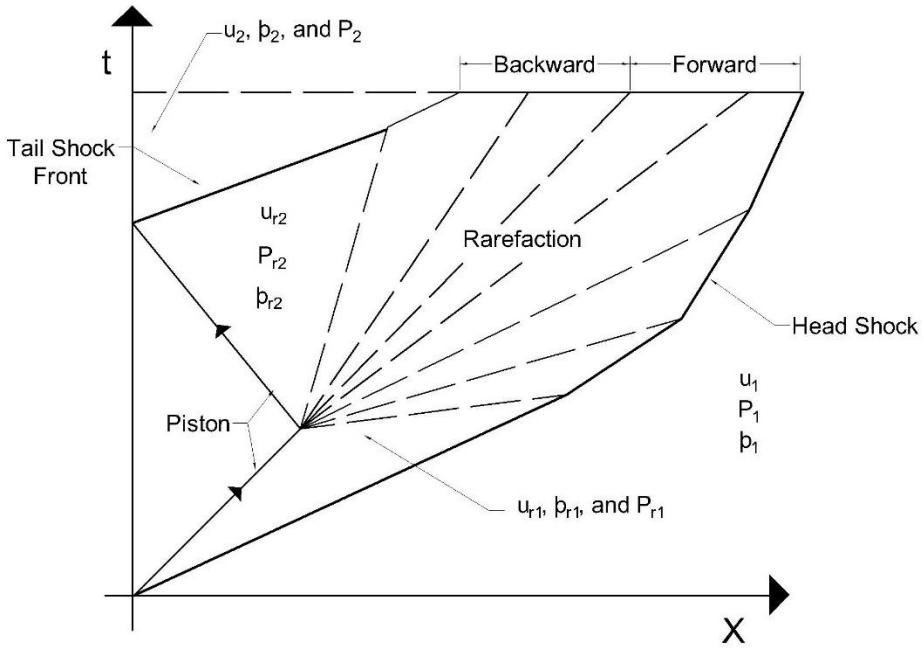

FIGURE 3.6 Decaying of N-Wave–Due to overtaking of head shock by forward rarefaction and tail shock overtaking backward rarefaction.

Source (Courant & Friedrichs, 1948)

3.5.1 Shock Wave Overtaken by A Rarefaction Wave

Figure 3.7 shows a schematic representation of planar shock overtaken by a weak rarefaction wave . Interaction can result in the following two wave patterns: a reflected rarefaction wave, or a reflected shock, while the transmitted wave in both case is a shock. As this transmitted wave decays with interactions, it strength decreases, and the entropy diminishes. Glass, et. al., 1959 presented algebraic equations relating the pressures ratios across transmitted and reflected wave (at the end of interactions) to the known values of pressure ratios across the incident shock and overtaking rarefaction wave (before interactions). When overtaking rarefaction wave is weak, the interaction results in a reflected rarefaction wave, the quasi-steady flow in regions (b) and (c) can be evaluated using expression (3.27) and (3.28) (Igra, 2001). The case of transmitted compression wave was tactically assumed. Hence it would not influence the terminal states and can be neglected (Glass, Heuckroth, & Molder, 1959).

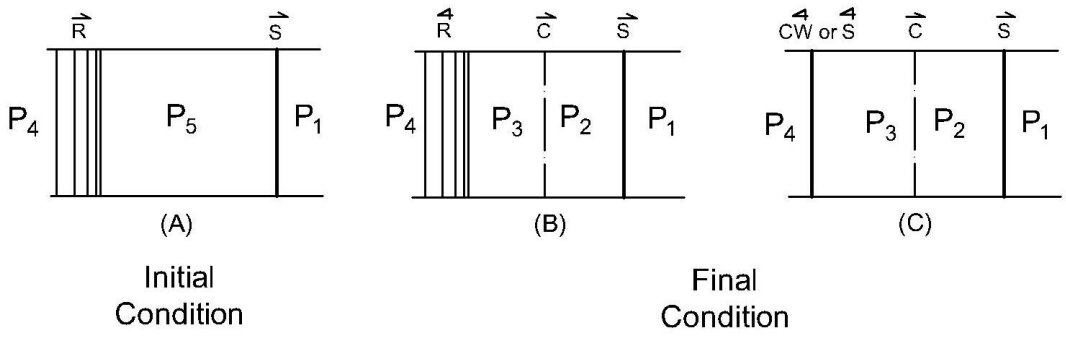

FIGURE 3.7: Overtaking of a Shock by a Weak Rarefaction Wave. (a) A shock of known strength overtaken by a rarefaction wave. (b) Flow field resulting from interaction can result into a transmitted shock wave with a reflected rarefaction or (c) a transmitted shock with a reflected wave that can be a shock or a compression wave

Source (Glass et al., 1959)

$$\sqrt{\frac{\beta\frac{P_1}{P_5}\left(\alpha+\frac{P_1}{P_5}\right)}{\left(1+\alpha\frac{P_1}{P_5}\right)}}\left[\frac{1-\frac{P_1}{P_5}}{\sqrt{\frac{P_1}{P_5}\left(\alpha+\frac{P_1}{P_5}\right)}}+\frac{1-\frac{P_2}{P_1}}{\sqrt{\alpha\frac{P_2}{P_1}+1}}\right] \tag{3.27}$$

$$+2\left(\frac{P_4}{P_5}\right)^{\beta}-\left(\frac{P_2}{P_1}\frac{P_1}{P_5}\right)^{\beta}-1=0$$

And

$$\left(\frac{P_3}{P_4}\right)=\frac{P_2}{P_1}\frac{P_1}{P_5}\frac{P_5}{P_4} \tag{3.28}$$

Where, $\beta=\frac{\gamma-1}{2\gamma}$ and $\alpha=\frac{\gamma+1}{\gamma-1}$

3.5.2 Shock Wave Overtaking A Rarefaction Wave

Figure 3.8 shows a schematic representation shock overtaking a rarefaction. A relatively weak shock of known strength proceeds from left to right and a rarefaction wave of known strength proceeds in a same direction. Interaction results into a reflected wave and a transmitted wave. The reflected wave can be a shock or a rarefaction wave while transmitted wave is a rarefaction wave. In the limiting case of a very weak shock, the overtaking shock wave is weakened until it is decayed to a Mach wave (Igra, 2001). Mach wave is the envelope of wave front, travelling at sound speed propagated from an infinitesimal disturbance in supersonic speed. For a weak incident shock wave, (a case when it completely attenuated to a Mach wave), the reflected wave is a shock wave, the quasi-steady flow in the regions (b) and (c) in figure 3.8 can be evaluated using (3.29) and (3.30) (Bremner, Dukowicz, & Glass, 1960).

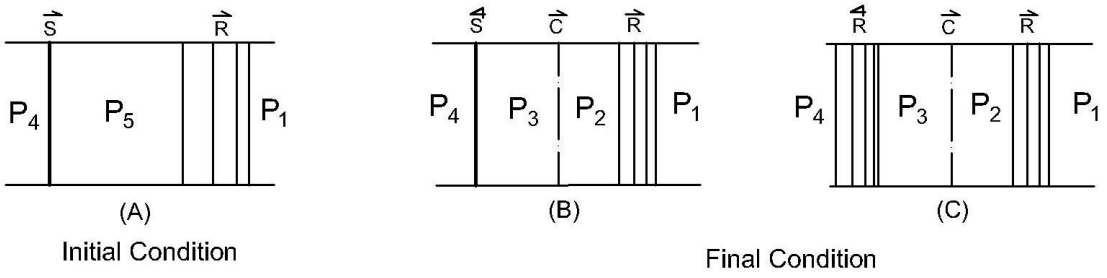

Figure 3.8: Shock Wave Overtaken by a Rarefaction Wave. (a) A shock of known strength overtaking a rarefaction wave. (b) Flow field resulting from interaction can result into a reflected shock wave with a reflected rarefaction or (c) reflected and transmitted wave both are rarefaction wave.

Source (Bremner et al., 1960)

$$\frac{1-\left(\frac{P_3}{P_4}\right)^{\beta}\left(\frac{P_4}{P_5}\right)^{\beta}}{\sqrt{\beta}}+\frac{\left(\frac{P_4}{P_5}-1\right)}{\left[1+\alpha\left(\frac{P_4}{P_5}\right)\right]^{1/2}} + \left[\frac{\frac{P_4}{P_5}\left(\alpha+\frac{P_4}{P_5}\right)}{1+\alpha\frac{P_4}{P_5}}\right]^{1/2}\frac{\left(1-\frac{P_4}{P_5}\right)}{\left[1+\alpha\frac{P_4}{P_5}\right]^{1/2}}=0 \tag{3.29}$$

And

$$\left(\frac{P_3}{P_4}\right)=\frac{P_2}{P_2}\frac{P_1}{P_5}\frac{P_5}{P_4} \tag{3.30}$$

Where, $\beta=\frac{\gamma-1}{2\gamma}$ and $\alpha=\frac{\gamma+1}{\gamma-1}$

Based on the above discussion, for a head shock overtaken by forward part of rarefaction $\left(\frac{P_1}{P_r}<1\right)$, the resulting flow field can be evaluated using equation (3.27) and (3.28):

$$\sqrt{\frac{\beta\frac{P_1}{P_{r1}}\left(\alpha+\frac{P_1}{P_{r1}}\right)}{\left(1+\alpha\frac{P_1}{P_{r1}}\right)}}\left[\frac{1-\frac{P_1}{P_{r1}}}{\sqrt{\frac{P_1}{P_{r1}}\left(\alpha+\frac{P_1}{P_{r1}}\right)}}+\frac{1-\frac{P_{r12}}{P_1}}{\sqrt{\alpha\frac{P_{r12}}{P_1}+1}}\right]$$

$$+2\left(\frac{P_r}{P_{r1}}\right)^{\beta}-\left(\frac{P_{r12}}{P_1}\frac{P_1}{P_{r1}}\right)^{\beta}-1=0$$

And

$$\left(\frac{P_{r13}}{P_r}\right)=\frac{P_{r12}}{P_1}\frac{P_1}{P_{r1}}\frac{P_{r1}}{P_r}$$

Using above expression, $P_{r12}=101{,}269Pa\ and\ P_{r13}=101{,}269Pa$ (see Appendix A)

Similarly, using equation (3.29) and (3.30), for evaluating flow field resulting from interaction for tail shock wave overtaking back ward part of rarefaction wave$\left(\frac{P_r}{P_2}<1\right)$:

$$\frac{1-\left(\frac{P_{r23}}{P_2}\right)^{\beta}\left(\frac{P_2}{P_{r2}}\right)^{\beta}}{\sqrt{\beta}}+\frac{\left(\frac{P_2}{P_{r2}}-1\right)}{\left[1+\alpha\left(\frac{P_2}{P_{r2}}\right)\right]^{1/2}}$$

$$+\left[\frac{\frac{P_2}{P_{r2}}\left(\alpha+\frac{P_2}{P_{r2}}\right)}{1+\alpha\frac{P_2}{P_{r2}}}\right]^{1/2}\frac{\left(1-\frac{P_{r23}}{P_2}\right)}{\left[1+\alpha\frac{P_{r23}}{P_2}\right]^{1/2}}$$

And

$$\left(\frac{P_{r23}}{P_2}\right)=\frac{P_{r22}}{P_r}\frac{P_r}{P_{r2}}\frac{P_{r2}}{P_2}$$

Using above expression $P_{r12}=100{,}527Pa\ and\ P_{r13}=100{,}527Pa$ (see Appendix A)

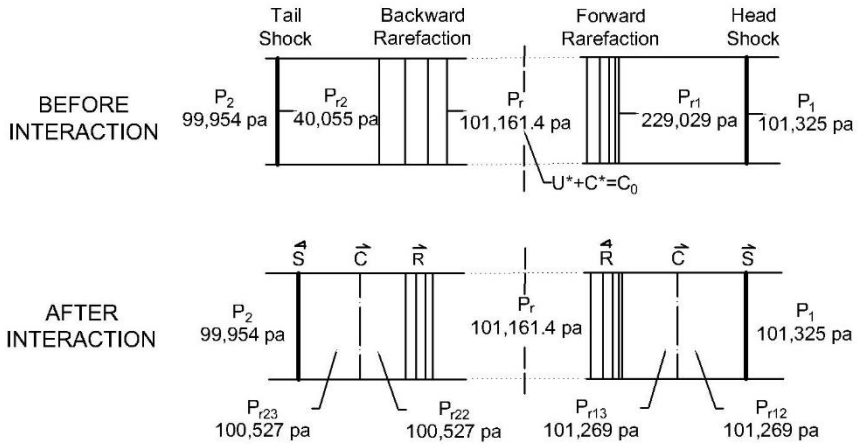

FIGURE 3.9 Flow Field Resulting from Interactions. Pressure jump across the head and tail shock diminishes due to interactions, resulting in decaying of wave energy.

The flow field shows resulting pressure across states (P_{r12}- P_{r22}) and transmitted shocks (P_1), after the interaction of head shock and forward rarefaction are almost identical, this means forward rarefaction has attenuated the head shock to Mach wave, just as its tail reaches the head shock. Similarly, in the case of tail shock overtaking the backward rarefaction, states (Pr_{22}- P_{r23}) and (P_2) are nearly coincident, thus, incident tail shock has been attenuated to a Mach wave, just as it reaches the head of the backward rarefaction (Bremner et al., 1960). Shocks keep on decaying during these interactions with the rarefaction waves, its strength (the pressure jumps across it) diminishes. Thus, at some distance from source, both the shock at head and tail of N-wave will get attenuated to Mach waves and will become one of the Mach line of rarefaction wave. As entropy across the shock continues to decay due to interactions with the rarefaction, there is reduction waveform speed and amplitude. This reduction is due to the dissipation of ultrasound energy. The loss of ultrasound energy and conservation of energy implies this energy is conserved and is transferred from one form to another. In this case, it becomes heat.

A similar set of calculation are performed for transducer of power levels of 50W, 150W, 500W and 1500W and for frequencies of 20kHz, 500kHz and 2MHz, as shown in table 3.1 and 3.2

Table 3.1 Vibration speed of Fluid Particle in Acoustic Field of Varying Power Level and Frequency

Power level, W (watt)	Frequency, f (kHz)	Intensity, I (W/m^2)	Amplitude, A (m)	Particle Speed, V (m/s)
1500	20	9477702.96	1691E-06	212.4
1500	500	9477702.96	67.6E-06	212.4
1500	2000	9477702.96	16.9E-06	212.4
500	20	3152941.98	976.3E-06	122.6
500	500	3152941.98	39.1E-06	122.6
500	2000	3152941.98	9.76E-06	122.6
150	20	94772.6	534.7E-06	67.2
150	500	94772.6	21.4E-06	67.2
150	2000	94772.6	5.34E-06	67.2
50	20	315924.2	308.7E-06	38.78
50	500	315924.2	12.3E-06	38.78
50	2000	315924.2	3.08E-06	38.78

Table 3.2 Variation in Resulting Flow Field

Particle speed, V (m/s)	P_1 (Pa)	P_{r1} (Pa)	P_r (Pa)	P_{r2} (Pa)	P_2 (Pa)	$P_{r12}=P_{r13}$ (Pa)	$P_{r22}=P_{r23}$ (Pa)	Head Shock, U_1 (m/s)
212.4	101325	229029	101161	40055	99954	101269	100527	490.8
122.6	101325	164678	102005	60027	101058	102004	101152	421.7
67.2	101325	132853	102220	76414	101281	102228	101294	383
38.7	101325	118629	102258	86225	101317	102260	101319	364

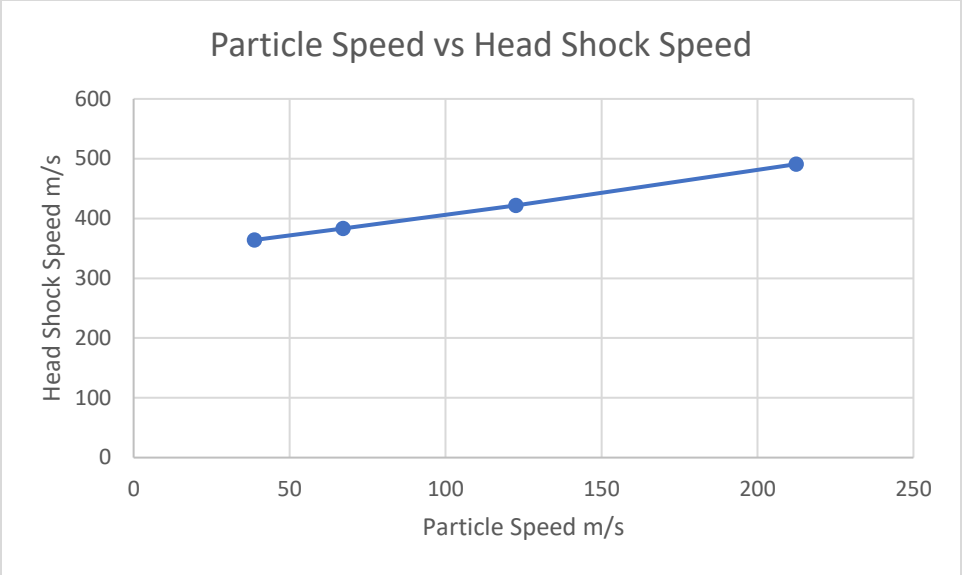

FIGURE 3.10 Particle Speed vs Head Shock. The speed of head shock and thereby strength of shock increases with increase in the disturbance speed of transducer.

3.6 Discussions of Results

In an ideal fluid (medium of propagation), displacement amplitude of an intense ultrasonic wave decreases with an increase in frequency of transducer, since amplitude is inversely proportional to the intensity of disturbance or vibration. But the vibration speed, remains constant for a given power level for different frequencies as shown in table 3.1. The strength of shock (discontinuity) that develops in waveform depends on the disturbance speed, higher the vibration speed stronger the discontinuity. For example, for particle speed of 212.4m/s strength of head shock is P_{r1}/P_1 is 2.26 whereas for particle speed of 122.6m/s it is 1.625. Similarly, it can be seen from pressure distribution in resulting flow field (before interaction), distortion in wave will also be increase with increase in power level. After the interaction, the shock strength (the pressure jumps across it) diminishes. For instance, for particle speed of 212.4 m/s pressure jump across head shock was 2.26 before interaction

and reduces to near atmospheric after the interactions. This causes dissipation of ultrasound energy, but since energy is conserved, it is transferred from one form to another. In this case, it becomes heat.

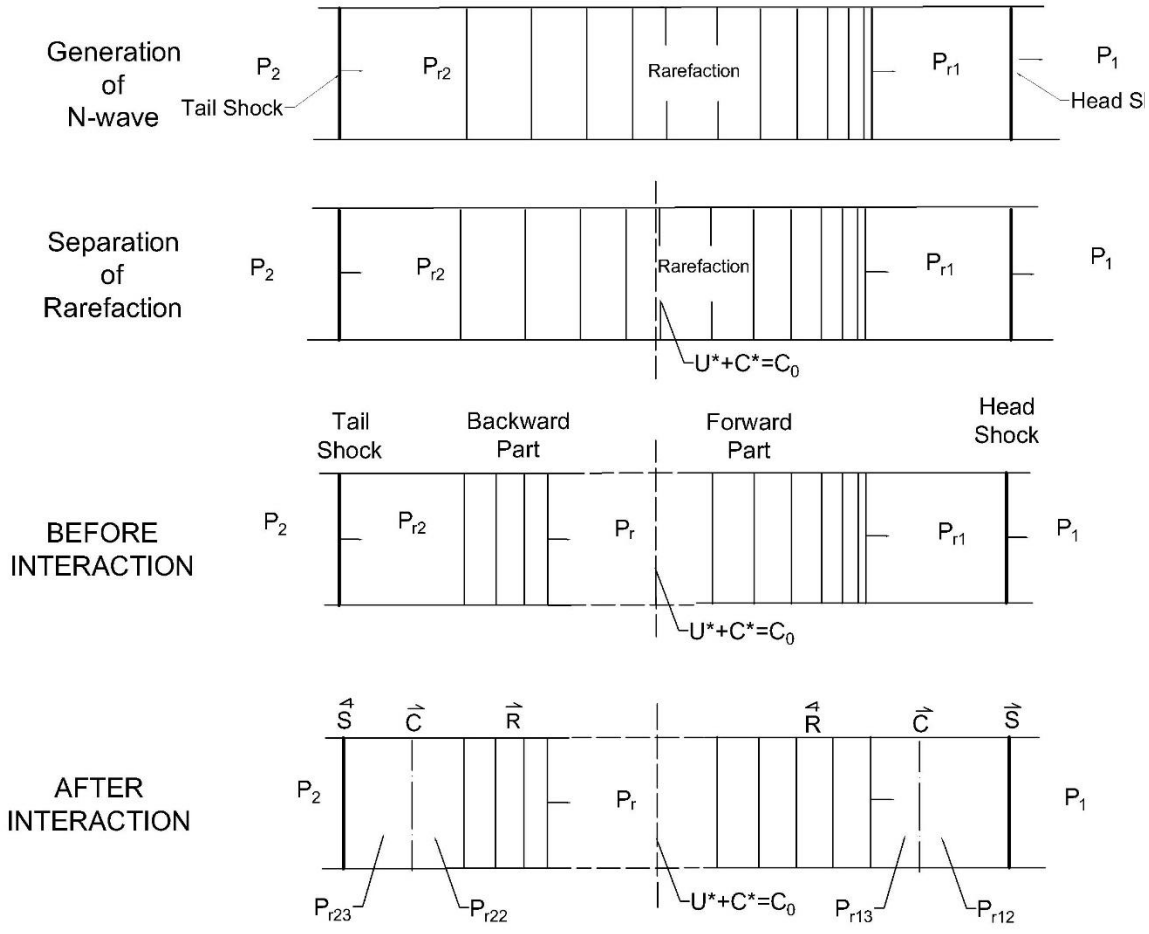

FIGURE 3.11 Intial & Final Condition of N-Wave. (a) In a pulse of intense ultrasonic wave two shocks will form with a rarefaction wave in between due to nonlinear wave motion of the wave. (b) Rarefaction can be divided into two parts separated by the sound wave, $u_* + c_* = c_0$. (c) Head shock traverses the forward part of rarefaction wave, the tail shock backward part. (d) Interaction results in decaying of shocks to a Mach wave.

CHAPTER 4
SUMMARY & CONCLUSION

In linear acoustics, disturbances always propagate at a constant speed relative to the medium and do not influence the fluid properties or behavior. The situation changes, dramatically, if the wave intensity is increased. Familiar laws like superposition, reflection, and refraction cease to be valid. Local sound speed changes from c_0 to $c_u + u$. Thus, with acoustic nonlinearity, there is different propagation velocities in different regions of a waveform hence shocks (discontinuities) are formed

In this research, one-dimensional motion of an ideal fluid is used to study the nonlinear propagation of intense acoustic waves. With a pulse of high-intensity wave, two shocks are formed at the boundaries and a rarefaction zone of varying velocity are also form in between them. The strength of shock will depend on the power level of the source, higher the power level produces stronger discontinuity. The wave speed at the face of the rarefaction zone is faster than that of the shock at the front, while the shock at back is travelling at a faster speed than that of the tail of the rarefaction zone. The rarefaction can be separated into two zones separated by the sound wave, $c_u + u = c_0$. The forward zone will overtake the shock at the front, while the tail shock overtakes the backward part. The pressure jump across the shocks will continue to decay during these interactions. The interactions will cause attenuation of the shock to a Mach wave and change in the entropy across the shock also diminish. This results in the dissipation of the shock's energy. Since energy is conserved, it is transferred from wave energy to heat.

These research helps to understand the nonlinear behavior of intense ultrasonic waves and can be used to model the processes involving the propagation of ultrasonic waves.

CHAPTER 5

SUGGESTION FOR FUTURE WORK

Nonlinear acoustic waves containing shocks can create wide range of mechanisms such as heating, agitation, diffusion, friction, mechanical rupture, and chemical effects. In this research, an attempt is made to understand the formation of shocks within intense waves and the decaying of shocks due sound-sound interactions within N-waves. However, in this study, the medium of propagation was an ideal fluid. It is proposed to extend the scope of this research to include the propagation of intense acoustic waves in non-ideal media, such as water, this will help to better understand the interactions of wave with the fluids. The shock will not appear immediately near the source, but will form at some distance from it, and the shock will continue to decay along the direction of propagation. Determining the distance from the source at which the shock appears and until when it decays will be essential to improving the applications of intense ultrasound.

APPENDIX A

MATLAB CODES

MATLAB coding to calculate pressure, $P_{r12}\ and P_{r13}$ for the case of the head shock wave overtaken by a forward region of rarefaction wave.

```
syms pr12
p1=101325;
pr1=229030;
pr=101161.4;
alpha=6;
beta=0.142857;
x=2*power((pr/pr1),beta);
b=(1-(pr12/p1))/(sqrt((alpha*(pr12/p1))+1));
a=(1-(p1/pr1))/sqrt((p1/pr1)*(alpha+(p1/pr1)));
c=sqrt(((beta*(p1/pr1))*((p1/pr1)+alpha))/((alpha*(p1/pr1))+1));
d=power((pr12/p1)*(p1/pr1),beta);
eqn=c*(a+b)+x-d-1==0;
solpr12= solve(eqn,pr12)


pr13=pr*(pr12/p1)*(p1/pr1)*(pr1/pr)
```

MATLAB coding to calculate pressure, $P_{r22}\ and P_{r23}$ for the case of the tail shock wave overtaking a backward region of rarefaction wave.

```
syms Pr23
P1=101161.4;
P5=40054.54;
P4=99953.85;
alpha=6;
beta=0.142857;
a=((1-((power((P3/P4),beta))*(power((P4/P5),beta))))/(sqrt(beta)));
b=(((P4/P5)-1)/(sqrt(1+(alpha*(P4/P5)))));
c2=((1-(P3/P4))/(sqrt(1+(alpha*(P3/P4)))));
c1=(sqrt(((P4/P5)*(alpha+(P4/P5)))/(1+(alpha*(P4/P5)))));
eqn=a+b+(c1*c2)==0
solPr23=solve(eqn,Pr23)

pr22=(pr23/p2)*pr*(pr2/pr)*(p2/Pr2)
```

APPENDIX B

MATLAB CODE FOR EQUATION OF STATE OF WATER

In this research, initial attempt was made to develop the proposed theory for water as medium of propagation. To expand this theory to water as medium, it was essential to have equation of state i.e., formulation to relate the thermodynamic properties of fluid phases of water over a wide range of conditions. International Association for the Properties of Water and Steam, IAPWS developed a formulation for the calculation of thermodynamic properties of ordinary water, this formulation is for calculating the free energy (Φ) as a function of temperature (T) and density (ρ); appropriate combinations of derivatives of expression can produce any thermodynamic property desired (sound speed, density, etc.) (IAPWS, 2016). An MATLAB coding was developed to calculate the free energy for a given density and temperature.

The equation is expressed in dimensionless form, $\Phi = f/RT$, and is separated into two parts, an ideal-gas part Φ^0 and a residual gas part Φ^τ:

$$\frac{f(\rho,T)}{RT} = \Phi(\delta,\tau) = \Phi^0(\delta,\tau) + \Phi^\tau(\delta,\tau)$$

Where, $\delta = \rho/\rho_c$ and $\tau = T_c/T$ with $T_c = 647.096K$, $\rho_c = 322kg\ m^{-3}$ and R = 0.46,151,805 Kj$kg^{-1}K^{-1}$

The ideal-gas part and residual gas-part can be calculated using following expression:

$$\phi^o = \ln\delta + n_1^o + n_2^o\tau + n_3^o \ln\tau + \sum_{i=4}^{8} n_i^o \ln\left[1 - e^{-\gamma_i^o \tau}\right]$$

$$\phi^r = \sum_{i=1}^{7} n_i \delta^{d_i} \tau^{t_i} + \sum_{i=8}^{51} n_i \delta^{d_i} \tau^{t_i} e^{-\delta^{c_i}} + \sum_{i=52}^{54} n_i \delta^{d_i} \tau^{t_i} e^{-\alpha_i (\delta-\varepsilon_i)^2 - \beta_i (\tau-\gamma_i)^2} + \sum_{i=55}^{56} n_i \Delta^{b_i} \delta\psi$$

with $\Delta = \theta^2 + B_i \left[(\delta - 1)^2 \right]^{a_i}$

$$\theta = (1-\tau) + A_i \left[(\delta-1)^2 \right]^{\frac{1}{2\beta_i}}$$

$$\psi = e^{-C_i(\delta-1)^2 - D_i(\tau-1)^2},$$

MATLAB coding to calculate ideal-gas part:

```
T=input('Enter value of Temperature:');
rho=input('Enter value of Density:');
Tc= 647.096;
rhoc = 322;
sigma = (rho)/(rhoc);
tau = Tc/T;
Oni = xlsread('HFEValues','B5:B9');
OgammaI = xlsread('HFEValues','C5:C9');
On1= -8.3204464837497;
On2= 6.6832105275932;
on3= 3.00632;
free_energy=(log(sigma)+On1+On2*(tau)+on3*log(tau));
for index=1:5
free_energy=free_energy++(((Oni(index)*log(1-exp(-OgammaI(index)*tau)))))
end
```

TABLE 1 Numerical values of the coefficients and parameters of the ideal-gas part

i	n_i^o	γ_i^o	i	n_i^o	γ_i^o
1	–8.320 446 483 749 7	–	5	0.973 15	3.537 342 22
2	6.683 210 527 593 2	–	6	1.279 50	7.740 737 08
3	3.006 32	–	7	0.969 56	9.244 377 96
4	0.012 436	1.287 289 67	8	0.248 73	27.507 510 5

TABLE 2 Numerical values of the coefficients and parameters of the Residual-gas part

i	c_i	d_i	t_i	n_i
1	–	1	−0.5	$0.125\,335\,479\,355\,23 \times 10^{-1}$
2	–	1	0.875	$0.789\,576\,347\,228\,28 \times 10^{1}$
3	–	1	1	$-0.878\,032\,033\,035\,61 \times 10^{1}$
4	–	2	0.5	0.318 025 093 454 18
5	–	2	0.75	−0.261 455 338 593 58
6	–	3	0.375	$-0.781\,997\,516\,879\,81 \times 10^{-2}$
7	–	4	1	$0.880\,894\,931\,021\,34 \times 10^{-2}$
8	1	1	4	−0.668 565 723 079 65
9	1	1	6	0.204 338 109 509 65
10	1	1	12	$-0.662\,126\,050\,396\,87 \times 10^{-4}$
11	1	2	1	−0.192 327 211 560 02
12	1	2	5	−0.257 090 430 034 38
13	1	3	4	0.160 748 684 862 51
14	1	4	2	$-0.400\,928\,289\,258\,07 \times 10^{-1}$
15	1	4	13	$0.393\,434\,226\,032\,54 \times 10^{-6}$
16	1	5	9	$-0.759\,413\,770\,881\,44 \times 10^{-5}$
17	1	7	3	$0.562\,509\,793\,518\,88 \times 10^{-3}$
18	1	9	4	$-0.156\,086\,522\,571\,35 \times 10^{-4}$
19	1	10	11	$0.115\,379\,964\,229\,51 \times 10^{-8}$
20	1	11	4	$0.365\,821\,651\,442\,04 \times 10^{-6}$
21	1	13	13	$-0.132\,511\,800\,746\,68 \times 10^{-11}$
22	1	15	1	$-0.626\,395\,869\,124\,54 \times 10^{-9}$
23	2	1	7	−0.107 936 009 089 32
24	2	2	1	$0.176\,114\,910\,087\,52 \times 10^{-1}$
25	2	2	9	0.221 322 951 675 46
26	2	2	10	−0.402 476 697 635 28
27	2	3	10	0.580 833 999 857 59
28	2	4	3	$0.499\,691\,469\,908\,06 \times 10^{-2}$
29	2	4	7	$-0.313\,587\,007\,125\,49 \times 10^{-1}$
30	2	4	10	−0.743 159 297 103 41
31	2	5	10	0.478 073 299 154 80
32	2	6	6	$0.205\,279\,408\,959\,48 \times 10^{-1}$
33	2	6	10	−0.136 364 351 103 43
34	2	7	10	$0.141\,806\,344\,006\,17 \times 10^{-1}$
35	2	9	1	$0.833\,265\,048\,807\,13 \times 10^{-2}$
36	2	9	2	$-0.290\,523\,360\,095\,85 \times 10^{-1}$
37	2	9	3	$0.386\,150\,855\,742\,06 \times 10^{-1}$
38	2	9	4	$-0.203\,934\,865\,137\,04 \times 10^{-1}$
39	2	9	8	$-0.165\,540\,500\,637\,34 \times 10^{-2}$
40	2	10	6	$0.199\,555\,719\,795\,41 \times 10^{-2}$
41	2	10	9	$0.158\,703\,083\,241\,57 \times 10^{-3}$
42	2	12	8	$-0.163\,885\,683\,425\,30 \times 10^{-4}$
43	3	3	16	$0.436\,136\,157\,238\,11 \times 10^{-1}$
44	3	4	22	$0.349\,940\,054\,637\,65 \times 10^{-1}$
45	3	4	23	$-0.767\,881\,978\,446\,21 \times 10^{-1}$
46	3	5	23	$0.224\,462\,773\,320\,06 \times 10^{-1}$
47	4	14	10	$-0.626\,897\,104\,146\,85 \times 10^{-4}$
48	6	3	50	$-0.557\,111\,185\,656\,45 \times 10^{-9}$
49	6	6	44	−0.199 057 183 544 08
50	6	6	46	0.317 774 973 307 38
51	6	6	50	−0.118 411 824 259 81

i	c_i	d_i	t_i	n_i	α_i	β_i	γ_i	ε_i
52	–	3	0	$-0.313\,062\,603\,234\,35 \times 10^{2}$	20	150	1.21	1
53	–	3	1	$0.315\,461\,402\,377\,81 \times 10^{2}$	20	150	1.21	1
54	–	3	4	$-0.252\,131\,543\,416\,95 \times 10^{4}$	20	250	1.25	1

i	a_i	b_i	B_i	n_i	C_i	D_i	A_i	β_i
55	3.5	0.85	0.2	−0.148 746 408 567 24	28	700	0.32	0.3
56	3.5	0.95	0.2	0.318 061 108 784 44	32	800	0.32	0.3

MATLAB Coding for calculating Residual Energy Part

```
T=input('Enter value of Temperature:');
rho=input('Enter value of Density:');
Tc= 647.096;
rhoc = 322;
sigma = (rho)/(rhoc);
tau = Tc/T;
i = xlsread('research2017','A2:A57');
di7 = xlsread('research2017','C2:C8');
ti7 = xlsread('research2017','D2:D8');
ni7 =xlsread('research2017','E2:E8');
di51 = xlsread('research2017','C9:C52');
ti51 = xlsread('research2017','D9:D52');
ni51 =xlsread('research2017','E9:E52');
ci51 = xlsread('research2017','B9:B52');
di54 = xlsread('research2017','C53:C55');
ti54 = xlsread('research2017','D53:D55');
ni54 =xlsread('research2017','E53:E55');
alphai = xlsread('research2017','F53:F55');
betai = xlsread('research2017','G53:G55');
gammaI = xlsread('research2017','H53:H55');
Ei = xlsread('research2017','I53:I55');
ni56 =xlsread('research2017','E56:E57');
bi56 =xlsread('research2017','K56:K57');
Ci56 =xlsread('research2017','M56:M57');
Di56 =xlsread('research2017','N56:N57');
Bi56 =xlsread('research2017','L56:L57');
ai56 =xlsread('research2017','J56:J57');
Ai56 =xlsread('research2017','O56:O57');
theta = (1-tau)+dot(Ai56,((sigma-1)^2).^(1/(2*Bi56)));
delta = theta^2+dot(Bi56,((sigma-1)^2).^(ai56));
w=((-Ci56*(sigma-1)^2)-(Di56*(tau-1)^2));
C = exp((-Ci56*(sigma-1)^2)-(Di56*(tau-1)^2));


Residual_term_01=0;
for index=1:7
   Residual_term_01
=Residual_term_01+(ni7(index)*(sigma^(di7(index)))*(tau^(ti7(index))))
end
Residual_Term_02=0;
for index=1:44
```

```
Residual_Term_02=Residual_Term_02+(ni51(index)*(sigma^(di51(index)))*(tau^(ti51(i
ndex)))*(exp(-sigma^(ci51(index)))))
end
Residual_Term_03=0;
for index=1:3

Residual_Term_03=Residual_Term_03+((ni54(index))*(sigma^(di54(index)))*(tau^(ti54
(index)))*(exp((-alphai(index)*(sigma-Ei(index))^2)-betai(index)*(tau-
gammaI(index))^2)))
end
Residual_Term_04=0;
for index=1:2

Residual_Term_04=Residual_Term_04+((ni56(index))*(delta^(bi56(index)))*sigma*(C(
index)))
end
Residual_Energy=Residual_term_01+Residual_Term_02+Residual_Term_03+Residual_
term_04;
```

REFERENCES

ACI 228.2R. (2013). *Report on Nondestructive Test Methods for Evaluation of Concrete in Structures*.

Bishko, A. V., Samokrutov, A. A., & Shevaldykin, V. G. (2008). Ultrasonic Echo-Pulse Tomography of Concrete using Shear Waves Low-Frequency Phased Antenna Arrays. *17th World Conference on Non-Destructive Testing*.

Blackstock, D. T., & Hamilton, M. F. (1998). Progressive Waves in Lossless and Lossy Fluids. In M. F. Hamilton & D. T. Blackstock (Eds.), *Nonlinear Acoustics*. Academic press.

Blitz, J. (1971). *Ultrasonics Methods and Applications*. Butterworths.

Bremner, G. F., Dukowicz, J. K., & Glass, I. I. (1960). *On the One-Dimensional Overtaking of a Rarefaction Wave by a Shock Wave*.

Bukiet, B. (1988). Application of Front Tracking to Two-Dimensional Curved Detonation Fronts. *Society for Industrial and Applied Mathematics*, *9*, 80–99.

Coe, J., & Brandenberg, S. J. (2010). P -Wave Reflection Imaging of Submerged Soil Models Using Ultrasound. *Journal of Geotechnical and Geoenvironmental Engineering*, *136*(10), 1358–1367. https://doi.org/10.1061/(ASCE)GT.1943-5606.0000346

Collins, R., Zhu, J., Mills, R., & Boxall, J. (2016). Soil Saturation Detection from in Pipe Ultrasound Measurements. *19th World Conference on Non-Destructive Testing*.

Courant, R., & Friedrichs, K. O. (1948). *Supersonic Flow and Shock Waves*. (F. John, J. E. Marsden, & L. Sirvich, Eds.), *Springer*.

Gallego-Juárez, J. A., & Graff, K. F. (2015). Introduction to Power Ultrasonics. In J. A. Gallego-Juárez & K. F. Graff (Eds.), *Power Ultrasonics: Applications of High-Intensity Ultrasound* (pp. 1–6). Woodhead Publishing. https://doi.org/http://dx.doi.org/10.1016/B978-1-78242-028-6.00001-6

Ghosh, A. (2013). Calculating Displacement Amplitude of Ultrasonic Power Transducer. Retrieved from https://physics.stackexchange.com/q/53371

Glass, I. I., Heuckroth, L. E., & Molder, S. (1959). *On the One-Dimensional Overtaking of a Shock Wave by a Rarefaction Wave*.

Glaze, W., Kang, J. W., & Chapin, D. H. (1987). The Chemistry of Water Treatment Processes Involving Ozone, Hydrogen Peroxide and Ultraviolet Radiation. *Ozone Science Enginnering*, *9*.

Hambling, D. (2017). 7 Scientific Advanes that Came out of World War 1. Retrieved from https://www.popularmechanics.com/military/research/g1577/7-surprising-scientific-advances-that-came-out-of-world-war-i/

Henglein, A. (1987). Sonochemistry: Historical Development and Modern Aspects. *Ultrasonics*, *25*, 7–16.

IAPWS. (2016). International Association for the Properties of Water and Steam, IAPWS R6-95(2016). *Revices Release on the IAPWS Formulation 1995 for the Thermodynamic Properties of Ordinary Water Substance for General and Scientific User*.

Igra, O. (2001). One-Dimensional Interactions. In G. Ben-Dor, O. Igra, & E. Tov (Eds.), *Handbook of Shock Waves, Vol 02*.

Leighton, T. (2007). What is Ultrasound? *Progress in Biophysics and Molecular Biology*, *93*(1–3), 3–83. https://doi.org/10.1016/j.pbiomolbio.2006.07.026

Meegoda, J. N., Batagoda, J. H., & Aluthgun-hewage, S. (2017). Briefing : In situ Decontamination of Sediments using Ozone Nanobubbles and Ultrasound. *Journal of Environmental Engineering and Sciences*, *12*(1), 1–3. https://doi.org/10.1680/jenes.17.00006

Neis, U. (2015). The Use of Power Ultrasound for Wastewater and Biomass Treatment. In J. A. Gallego-Juárez & K. F. Graff (Eds.), *Power Ultrasonics: Applications of High-Intensity Ultrasound* (pp. 973–996). Woodhead Publishing. https://doi.org/http://dx.doi.org/10.1016/B978-1-78242-028-6.00032-6

Oelze, M., Darmody, R., & O'Brien, W. (2001). Measurement of Attenuation and Speed of Sound in Soils for the Purposes of Imaging Buried Objects. *The Journal of the Acoustical Society of America*, *109*(5), 2287–2287. https://doi.org/10.1121/1.4744005

Parson, S. A., & Williams, M. (2004). Introduction. In S. . Parson (Ed.), *Advanced Oxidation Processes for water and wastewater treatment* (pp. 1–6). IWA publishing.

Petrier, C. (2015). The Use of Power Ultrasound in Water. In J. A. Gallego-Juárez & K. F. Graff (Eds.), *Power Utrasonics: Applications of High-Intensity Ultrasound* (pp. 939–972). Woodhead Publishing. https://doi.org/http://dx.doi.org/10.1016/B978-1-78242-028-6.00031-4

Petrier, C., Lamy, M.-F., Francony, A., Benahcene, A., David, B., Renaudin, V., & Gondrexon, N. (1994). Sonochemical Degradation of Phenol in Dilute Aqueous Solutions: Comparison of the Reaction Rates at 20 and 487 kHz. *The Journal of Physical Chemistry*, *98*(41), 10514–10520. https://doi.org/10.1021/j100092a021

Pierce, A. D. (1994). Acoustics: An Introduction to its Physical Principle and Applications. NY: woodbury.

Pierce, A. D. (2002). Entropy, Acoustic, and Vorticity Mode Decomposition as an Intial step in Nonlinear Acoustic Formulations. In Rudenko & O. A. Sapozhnikov (Eds.), *Nonlinear Acoustics at the Beginning of the 21st Century* (pp. 11–19). Moscow State University.

Sapozhnikov, O. A. (2015). High-intensity Ultrasonics Waves in Fluids: Nonlinear Propagation and Effects. In J. A. Gallego-Juárez & K. F. Graff (Eds.), *Power Utrasonics: Applications of High-Intensity Ultrasound* (pp. 9–35). Woodhead Publishing. https://doi.org/http://dx.doi.org/10.1016/B978-1-78242-028-6.00002-8

Sehgal, C. M., & Wang, S. Y. (1981). Threshold Intensities and Kinetics of Sonoreaction of Thymine in Aqueous Solutions at Low Ultrasonic Intensities. *Journal of American Chemical Society*. https://doi.org/10.1002/chin.198207122

Sivasankar, T., & Moholkar, V. S. (2009). Physical insights into the sonochemical degradation of recalcitrant organic pollutants with cavitation bubble dynamics. *Ultrasomics Sonochemical*, *16*, 769–781.

Tiehm, A., Nickel, K. Z., & Neis, U. (2001). Ultrasonic waste activated sludge disintegration for improving anaerobic stabilization. *Water Res.*, *35*(8), 2003–2009.

Wood, R. W., & Loomis, A. L. (1927). The Physical and Biological Effects of High-Frequency Sound-Waves of Great Intensity. *The London, Edinburgh, and Dublin Philosophical Magazine and Journal of Science*, *4*(22), 417–436. https://doi.org/10.1080/14786440908564348